Received: 18 January 2021 | Revised: 12 June 2021 | Accepted: 14 June 2021

DOI: 10.1111/cas.15032

ORIGINAL ARTICLE

Cancer Science WILEY

Lack of GD3 synthase (St8sia1) attenuates malignant properties of gliomas in genetically engineered mouse model

Yuki Ohkawa[1,2] | Pu Zhang[1,3] | Hiroyuki Momota[4,5] | Akira Kato[4] | Noboru Hashimoto[3] | Yuhsuke Ohmi[1] | Robiul H. Bhuiyan[1] | Yesmin Farhana[1,3] | Atsushi Natsume[4] | Toshihiko Wakabayashi[4] | Keiko Furukawa[1] | Koichi Furukawa[1,3]

[1]Department of Biomedical Sciences, Chubu University College of Life and Health Sciences, Kasugai, Japan

[2]Department of Glyco-Oncology and Medical Biochemistry, Osaka International Cancer Institute, Osaka, Japan

[3]Department of Biochemistry II, Nagoya University Graduate School of Medicine, Nagoya, Japan

[4]Department of Neurosurgery, Nagoya University Graduate School of Medicine, Nagoya, Japan

[5]Department of Surgical Neuro-Oncology, The Institute of Medical Science, University of Tokyo, Tokyo, Japan

Correspondence
Koichi Furukawa, Department of Biomedical Sciences, Chubu University College of Life and Health Sciences, Kasugai, Japan.
Email: koichi@isc.chubu.ac.jp

Funding information
Ministry of Education, Culture, Sports and Technology of Japan, Grant/Award Numbers: 15H04696, 25670141, 24390078, 23110008, 20K07629; JST-CREST, Grant/Award Number: JPMJCR17H2.

Abstract

High expression of gangliosides GD3 and GD2 is observed in human gliomas. The functions of GD3 and GD2 in malignant properties have been reported in glioma cells in vitro, but those functions have not yet been investigated in vivo. In this study, we showed that deficiency of GD3 synthase (GD3S, St8sia1) attenuated glioma progression and clinical and pathological features in a platelet-derived growth factor B-driven murine glioma model. Lack of GD3S resulted in the prolonged lifespan of glioma-bearing mice and low-grade pathology in generated gliomas. Correspondingly, they showed reduced phosphorylation levels of Akt, Erks, and Src family kinases in glioma tissues. A DNA microarray study revealed marked alteration in the expression of various genes, particularly in MMP family genes, in GD3S-deficient gliomas. Re-expression of GD3S restored expression of *MMP9* in primary-cultured glioma cells. We also identified a transcription factor, Ap2α, expressed in parallel with GD3S expression, and showed that Ap2α was critical for the induction of *MMP9* by transfection of its cDNA and luciferase reporter genes, and a ChIP assay. These findings suggest that GD3S enhances the progression of gliomas by enhancement of the Ap2α-MMP9 axis. This is the first report to describe the tumor-enhancing functions of GD3S in vivo.

KEYWORDS

ganglioside, glioma, knockout, matrix metalloproteinase, sialyltransferase

1 | INTRODUCTION

Gliomas are brain tumors derived from mostly glial cells.[1] Gliomas are classified into four histological grades, and the highest grade glioma, glioblastoma multiforme (grade IV), is a tumor associated with one of the poorest prognoses in adults.[2] Gliomas are also classified into three subtypes, mesenchymal, proneural, and classical, according to gene expression profiles.[3] Loss of function of p53 and

Abbreviations: GD3S, GD3 synthase (ST8SIA1); GFAP, glial fibrillary acidic protein; GO, gene ontology; PDGFB, platelet-derived growth factor B; PDGFR, platelet-derived growth factor receptor; RCAS, replication-competent avian leukemia virus splice acceptor; SFK, Src family kinase.

overexpression of PDGFRα have been frequently identified in the proneural subtype.

Gangliosides GD3 and GD2 are acidic glycosphingolipids, and are expressed in some types of tumors such as melanomas, gliomas, and small-cell lung cancers.[4–6] As expression of GD3 and GD2 is high and specific for these tumors, they are considered cancer-associated antigens and suitable as targets of immune therapies.[7] Previously, we reported that ganglioside GD3 enhanced PDGFRα-mediated signals by forming a ternary complex consisting of GD3, PDGFRα, and Yes kinase in lipid rafts of the plasma membrane, leading to marked invasiveness of glioma cells in vitro.[8] However, no studies on the roles of GD3 in actual glioma tissues in the body have been reported.

Replication-competent avian leukemia virus splice acceptor vector allows specific delivery of oncogenes to astrocyte-lineage cells using Gtv-a transgenic mice that express tv-a, an avian leukemia virus receptor, under regulation of a GFAP promoter.[9] This is one of the murine cancer models produced by genetic engineering.[10] In this system, cDNA transfection of PDGFB by RCAS into cortexes of Gtv-a mice results in the generation of gliomas in a few weeks.

In this study, we clarified how GD3 and GD2 are involved in glioma progression in vivo using an RCAS system. We compared gliomas generated in GD3S-WT mice and those in GD3S-KO mice. Here, we show that the lack of GD3S attenuated tumor properties of gliomas by modulating expression of various genes in vivo. Key molecules involved in the malignant properties of gliomas under GD3S expression were investigated.

2 | MATERIALS AND METHODS

2.1 | Mice

A Gtv-a transgenic mouse that expresses tv-a under a GFAP promoter was obtained from Jackson Laboratory. The Tp53 KO mouse was obtained from Riken Bioresource Center. The GD3S-KO mouse was generated in our laboratory.[11] By crossing Gtv-a mice with p53 KO and GD3S KO mice, Gtv-a$^{+/+}$/Tp53$^{-/-}$/GD3S$^{+/+}$ and Gtv-a$^{+/+}$/Tp53$^{-/-}$/GD3S$^{-/-}$ mice were generated. Original genetic backgrounds of these mice were: Gtv-a (129, BALB/c, FVB/N, C57BL/6), p53-KO (C57BL/6), and GD3S-KO (C57BL/6).

2.2 | Generation of glioma-bearing mice

For the preparation of virus-producing cells, DF-1 cells (a chicken embryonic fibroblast cell line) were transfected with an RCAS vector harboring PDGFB-T2A-GFP cDNA by Lipofectamine 2000™ (Invitrogen), and virus-producing DF-1 cells (1×10^4) were injected into the right cortexes of newborn mice by Hamilton syringe (21 G). At 7 or 14 days after injection, mice were killed with carbon dioxide gas, and brains with gliomas were harvested and imaged by IVIS Spectrum (PerkinElmer). Brains with gliomas were analyzed by H&E staining, and also used for the preparation of primary-cultured glioma cells. DF-1 cells and virus-producing DF-1 cells were maintained in DMEM supplemented with 10% FCS, penicillin, and streptomycin in a CO_2 incubator at 37°C.

2.3 | Preparation of primary-cultured astrocytes and glioma cells

Brains from newborn mice or glioma tissues from mice harboring gliomas were harvested, and brains or glioma tissues were passed through a mesh (pore size, 200 μm) after removing meninges. After washing cells with PBS, they were cultured in DMEM supplemented with 10% FCS and antibiotics. To remove contaminated microglia, trypsinized cells were plated on Petri dishes and incubated for 20 minutes. Microglia attached to Petri dishes better than astrocytes. Therefore, the majority of unattached cells after incubation for 20 minutes were astrocytes. We repeated this procedure at least three times to remove microglia. To prepare primary cultured glioma cells, GFP-expressing cells were collected and enriched several times by FACS Aria II (Becton Dickinson).

2.4 | Western blot analysis

Lysates prepared from tissues (50 μg) or cells (20 μg) were separated by SDS-PAGE using 8, 10, or 12% acrylamide gels. After transferring proteins onto PVDF membranes (Millipore), the membranes were blocked with 5% skim milk in PBS containing 0.05% Tween-20. Incubation with primary Abs and subsequently with HRP-labeled secondary Abs was carried out, and the membranes were then analyzed with an ECL detection system (Wako) and C-Digit Blot Scanner (M&S TechnoSystems). Antibodies for Ap2α and GFP were purchased from Santa Cruz Biotechnology. Antibodies for 2A peptide, HA epitope, and β-actin were purchased from Sigma-Aldrich. Other Abs for Akt, phosphorylated Akt (S473), Erks, phosphorylated Erks, and phosphorylated SFKs (Y417) were purchased from Cell Signaling Technology, and Abs for individual gangliosides were established in our laboratory.[12]

2.5 | Microarray analysis

Pooled RNA samples of glioma tissues prepared from five each of GD3S-WT and GD3S-KO mice were analyzed by Agilent Expression Array (Agilent Technologies). The analysis of microarray results was carried out by Takara Bio.

2.6 | Quantitative RT-PCR

Extraction of total RNAs from tissues and cells and reverse transcription were carried out using TRIzol reagent (Invitrogen) and M-MLV reverse transcriptase (Invitrogen), respectively, according to the manufacturer's protocols. Complementary DNAs were analyzed

by SsoAdvanced Universal SYBR Green Supermix (Bio-Rad) and CFX Connect Real-Time PCR Detection System (Bio-Rad). The thermal cycle program recommended by Bio-Rad was used. Primers used in this study are listed in Table S1.

2.7 | Flow cytometry and cell sorting

Cells were trypsinized and washed twice with ice-cold PBS. For staining of GD3 and GD2, cells were incubated with an anti-GD3 Ab (R24, provided by Dr LJ Old, Sloan-Kettering Cancer Center) or an anti-GD2 Ab (220-51)[12] in PBS for 1 hour on ice. After washing with ice-cold PBS, cells were incubated with a phycoerythrin-labeled secondary Ab in PBS for 45 minutes on ice. Expression levels of GD3 and GD2 were analyzed by FACSCalibur (Becton Dickinson), and GD3-expressing cells were collected and enriched by FACSAria II (Becton Dickinson).

2.8 | Gelatin zymography

First, cells were cultured in Opti-MEM I (Thermo Fisher Scientific) supplemented with ITS (Thermo Fisher Scientific) for 2 days. Then the supernatant was collected and concentrated using Amicon Ultra-15 Filter Unit 30K (Merck Millipore). The supernatant containing 5 μg total protein was separated by SDS-PAGE including 1 mg/mL gelatin (Wako) under nonreducing conditions. After electrophoresis, the gel was washed with washing buffer (50 mmol/L Tris, pH 7.5, 2.5% v/v Triton X-100, 5 mmol/L $CaCl_2$, and 1 μmol/L $ZnCl_2$) and incubated with incubation buffer (50 mmol/L Tris, pH 7.5, 1% v/v TritonX-100, 5 mmol/L $CaCl_2$, and 1 μmol/L $ZnCl_2$) overnight at 37°C. To visualize the gelatinase activity, the gel was stained with GelCode Blue Stain Reagent (Thermo Fisher Scientific).

2.9 | Invasion assay

Matrigel (Corning) was diluted five times in PBS and added on a cell culture insert (24-well plate format, 8-μm pore size; Corning) and incubated for 2 hours at room temperature to be polymerized. After washing the insert, cells (2×10^3 in 200 μL serum-free DMEM) were plated onto the upper chamber. The lower chamber was filled with 700 μL DMEM supplemented with 10% FCS. After incubation in a CO_2 incubator at 37°C for 24 hours, invading cells were stained with Giemsa solution (Wako), and then the cell number was counted under microscopy (DMi1; Leica). Invading cells were also photographed with microscopy (BZ-X710; Keyence). For MMP9 inhibition, MMP9 inhibitor I (CAS No. 1177749-58-4; Sigma) was added into the upper chamber. The final concentration of MMP9 inhibitor I was 20 μmol/L.

2.10 | Chromatin immunoprecipitation

After washing with PBS, cells (1×10^7) were fixed with 1% formamide in PBS for 10 minutes and incubated with 0.125 mol/L glycine in PBS for 5 minutes. The cells were lysed by RIPA buffer (25 mmol/L Tris-HCl, pH 7.4, 150 mmol/L NaCl, 1% NP-40, 0.1% SDS, and 1% sodium deoxycholate) containing protein inhibitor cocktail (Calbiochem). The lysates were sonicated to fragment genomic DNA into approximately 600-1000 bp, and centrifuged at 20 630 *g* for 10 minutes to remove insoluble materials. After transferring the lysates to new tubes, immunoprecipitation was carried out with an anti-Ap2α Ab (sc-184; Santa Cruz Biotechnology) and Protein A Sepharose 4 Fast Flow (GE Healthcare). After washing three times with washing buffer (50 mmol/L Tris-HCl, pH 7.4, 1 mmol/L Na_3VO_4, 150 mmol/L NaCl, and 0.5% Triton X-100), the immunoprecipitates were heated in 500 μL Tris-EDTA at 95°C for 15 minutes. Then RNaseA (50 μg/mL; Sigma) treatment at 37°C for 30 minutes and Proteinase K (200 μg/mL; Sigma) treatment at 55°C for 1 hour were carried out. DNA purification was undertaken using phenol and chloroform by the standard method. Finally, ethanol precipitation was carried out to pellet DNAs, and the pellets were dissolved in 50 μL Tris-EDTA. Using these DNA solutions, PCR and quantitative PCR analyses were carried out. Primers used in this study are listed in Table S2.

2.11 | Luciferase assay

Two micrograms each of pcDNA3.1/Ap2α tv1 or pcDNA3.1/Ap2α tv3 and pGL3-Enhancer vector harboring the *MMP9* gene promoter sequence and pNL1.1TK vector (Promega) were used to transfect primary-cultured astrocytes (2×10^5) using ViaFect Transfection Regent (Promega). Cells were replated in white-bottom 96-well plates (2.5×10^4/well) after transfection. After culturing for 24 hours, the luminescence of the cells was measured by the Nano-Glo Dual-Luciferase Reporter Assay System (Promega) and a plate reader, Mithras LB-940 (Berthold).

2.12 | Preparation of frozen sections

At 14 days after injection of PDGFB-T2A-GFP cDNA-expressing cells by RCAS, brain tissues were harvested and fixed with 4% paraformaldehyde. After incubation at 4°C overnight, tissues were subsequently incubated in 10% sucrose for 8 hours, 15% sucrose for 8 hours, and 20% sucrose overnight. Tissues were then embedded in OCT compound (Sakura Finetek). Ten micrometer-thick frozen sections of brain tissues were prepared by a cryostat (Leica).

2.13 | Immunohistochemical analysis

Frozen sections were blocked with 1% BSA in PBS containing 0.075% Tween-20 for 1 hour. After washing with PBS, sections were incubated with primary Abs diluted in 1% BSA in PBS containing 0.01% Tween-20 for 1 hour. Then sections were washed with PBS and incubated with secondary Abs diluted in 1% BSA containing 0.01% Tween-20 for 1 hour. After washing with PBS, counterstaining with DAPI was carried out, and sections were mounted in 90% glycerol.

Expression patterns of gangliosides were observed under confocal microscopy (FV10i-LIV; Olympus Life Science).

2.14 | Study approval

All experimental protocols using mice were approved by the animal experimental committee of the Graduate School of Medicine in Nagoya University, adhering to the guidelines set by the Japanese government.

2.15 | Statistical analysis

Statistical analysis was undertaken using Student's *t* test. Kaplan-Meier analysis was carried out using the log-rank test.

3 | RESULTS

3.1 | Lack of GD3S attenuated tumor properties and progression of gliomas

First, to clarify whether GD3 and GD2 or GD3S are involved in glioma generation and progression, we analyzed gliomas generated in the RCAS/Gtv-a glioma model. To generate gliomas, we injected PDGFB-T2A-GFP cDNA-expressing cells into right cortexes of GD3S-KO glioma model mice or GD3S-WT (control) mice by the RCAS system (Figure 1A). T2A peptide is a self-cleaving small peptide derived from *Thosea asigna*.[13] The vector could express two genes linked by the T2A sequence at the same levels. By introducing this RCAS vector, gliomas expressing both PDGFB and GFP were generated. GD3S-KO mice showed a significantly longer life-span than control mice after injection ($P = .0228$, log-rank test) (Figure 1B). Based on the observation of GFP signals, GD3S-KO mice showed smaller gliomas than control mice at 2 weeks after injection (Figure 1C). Gliomas generated in GD3S-KO mice showed oligodendroglioma-like features, whereas those in control mice showed glioblastoma multiforme-like features in pathological analysis (Figure 1D). Immunohistochemical analysis revealed strong expression of GD3 and GD2 only in gliomas in control mice (Figures 1E and S1). More complex gangliosides than GD2 and a-series gangliosides showed similar staining patterns between gliomas and nonglioma tissues (Figure S1). These data suggest that GD3 and/or GD2 expression largely affects the nature of gliomas, and probably enhances glioma progression in vivo. Notably, in human gliomas, GD3 and GD2 expression could be enriched in the classical subtype, but there is no strong association with any subtype (Figure S2).

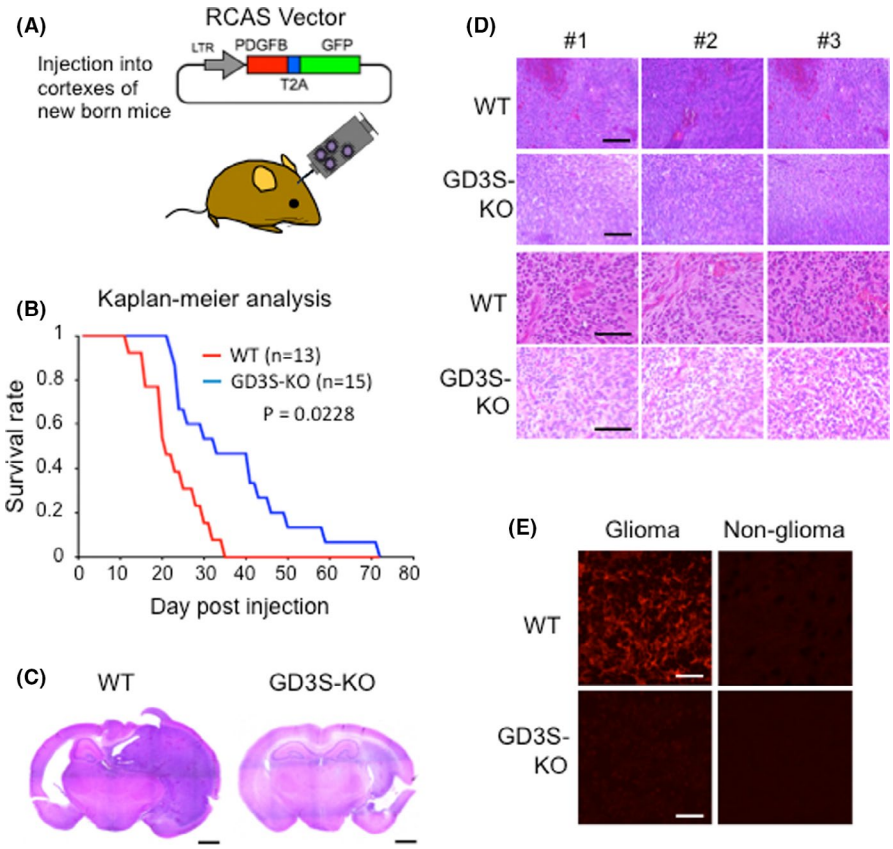

FIGURE 1 Lack of GD3 synthase (GD3S) attenuated glioma progression. A, Scheme showing the generation of gliomas in the replication-competent avian leukemia virus splice acceptor (RCAS)/Gtv-a glioma system. B, Survival rates of GD3S-KO and control mice after injection of PDGFB-T2A-GFP cDNA-expressing cells by RCAS. C, H&E staining of brains with gliomas at 2 wk after injection. Coronal section images of brains of GD3S-KO and control mice are shown. Bars, 1 mm. D, High-magnification images of H&E-stained brain sections harboring gliomas. Three representatives each of GD3S-KO and control mice are shown. Bars, 200 μm (upper panels), 50 μm (lower panels). E, Immunohistochemistry showing GD3 expression in gliomas and nonglioma regions (opposite site cortex) in GD3S-KO and control mice. Red indicates GD3 stained with anti-GD3 mAb and Alexa 546-conjugated anti-mouse IgGs. Bars, 40 μm. PDGFB, platelet-derived growth factor B

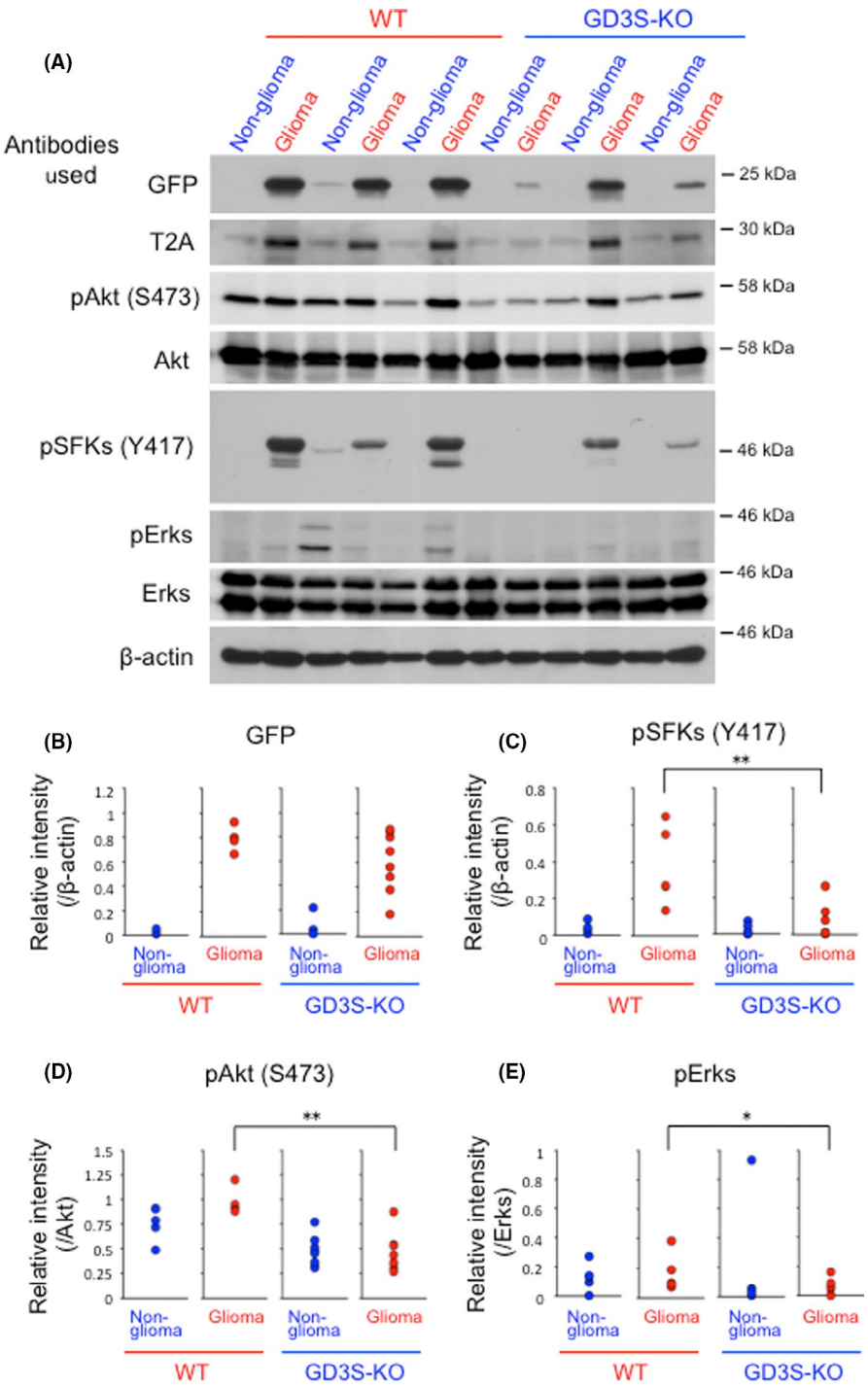

FIGURE 2 Lack of GD3 synthase (GD3S) attenuated phosphorylation levels of signaling molecules in gliomas. A, Two weeks after 2 wk of injection of PDGFB-T2A-GFP cDNA-expressing cells by replication-competent avian leukemia virus splice acceptor, lysates of glioma or nonglioma brain tissues were prepared and applied to western blotting. Total proteins (50 μg) were analyzed using Abs, as indicated on the left side of individual images. Representative results of three sample sets including GD3S-KO and control mice are shown. B-E, Relative expression levels of GFP (B), relative phosphorylation levels of Src family kinases (SFKs) (C), Akt (D), and Erks (E) are plotted. GFP expressions and phosphorylation levels of SFKs were normalized by β-actin bands. Phosphorylation levels of Akt and Erks were normalized by bands of total Akt and total Erks, respectively. Samples from seven GD3S-KO mice and five control mice were analyzed. $^{*}P < .05$, $^{**}P < .01$

3.2 | Lack of GD3S attenuated phosphorylation levels of Akt, Src family kinases, and Erks in glioma tissues

Next, we undertook western blot analysis using lysates prepared from gliomas generated in GD3S-KO mice and control mice at 2 weeks after the injection of PDGFB-T2A-GFP cDNA-expressing cells by RCAS. Nonglioma tissues were also prepared from the opposite site cortex of gliomas in the same mouse as the control. As shown in Figure 2, GFP and T2A expressions were restricted in gliomas. The T2A short peptide sequence worked as a tag protein for PDGFB. Therefore, anti-2A peptide Ab could detect exogenous PDGFB carrying the T2A peptide in its C-terminus. Interestingly, in glioma tissues, phosphorylation levels of Akt, SFKs, and Erks were significantly lower in GD3S-KO mice than in control mice. Generally, malignant gliomas show strong activation of signaling pathways of PI3K/Akt, SFK, and RAS/MAPK[14]; hence, these data indicate the lack of GD3/GD2 and/or GD3S attenuated oncogenic signals, leading to the generation of gliomas with low-grade malignancy.

Cell cycle

Gene	WT	GD3S-KO	Ratio
Apitd1	720.6	22.6	-4.99
Nuf2	597.9	97.7	-2.61
Cdkn2a	24683.2	4276.7	-2.53
Hmga2	1154.3	204.8	-2.50
Cdca2	37.1	6.6	-2.49
Cdkn2b	10443.9	2169.8	-2.27
Aurkb	119.6	30.6	-1.97
Ect2	255.6	67.4	-1.92
Mis18bp1	1,155.3	306.9	-1.91
Ccnd1	142502.2	37905.0	-1.91
Oip5	1339.0	364.4	-1.88
Nusap1	7247.9	1978.9	-1.87
Bub1b	2876.9	822.0	-1.81
Dlgap5	455.8	130.9	-1.80
Knstrn	2764.0	798.1	-1.79
Clspn	533.3	156.8	-1.77
Cdk1	262.0	77.0	-1.77
Ccnb1	1803.6	531.2	-1.76
Fam64a	5895.9	1761.2	-1.74
Sgol1	5436.2	1623.9	-1.74
Mastl	781.0	233.7	-1.74
Ect2	4239.2	1268.7	-1.74
Chtf18	3885.0	1170.5	-1.73
Aspm	6699.4	2020.5	-1.73
Ccne2	17.5	5.3	-1.72
Bub1	2512.8	766.2	-1.71
Cdca8	3824.5	1172.0	-1.71
Cntrl	164.9	51.3	-1.68
Ccnb2	20799.1	6486.9	-1.68
Cep55	149.7	47.4	-1.66
Birc5	5371.8	1714.4	-1.65
Cdc25c	1236.6	395.6	-1.64
Kif18b	1230.6	393.7	-1.64
Ube2c	14728.4	4718.9	-1.64
Gsg2	1575.5	505.5	-1.64
Irf1	17718.1	5689.2	-1.64
Cdca5	6,305.1	2030.2	-1.63
Foxm1	393.6	127.7	-1.62
Fanci	2151.3	700.9	-1.62
Fam83d	1322.3	436.1	-1.60
Cdca5	6680.3	2219.4	-1.59
Gas2l3	1633.4	544.2	-1.59
Cks2	1655.0	552.2	-1.58
Zwilch	5091.2	1700.7	-1.58
Anxa1	7042.5	2362.1	-1.58
Foxm1	2996.7	1015.1	-1.56
Chaf1b	9636.1	3277.5	-1.56
Cks1brt	827.9	282.5	-1.55
Ube2c	17408.0	5969.4	-1.54
Tpx2	6316.1	2166.4	-1.54
Cdc20	29213.1	10022.5	-1.54
Kif2c	1054.0	362.7	-1.54
Aurka	12491.9	4315.9	-1.53
Cdca2	1686.8	584.3	-1.53
Zwilch	2375.3	823.2	-1.53
E2f7	3246.2	1125.5	-1.53
Plk1	25145.5	8780.0	-1.52
Ccna2	16137.4	5649.8	-1.51

Extracellular matrix

Gene	WT	GD3S-KO	Ratio
MMP12	183.4	7.1	-4.69
MMP10	4865.2	392.0	-3.63
MMP9	985.0	81.8	-3.59
Ambn	61.1	6.2	-3.30
Adamts19	52.3	8.1	-2.69
Tecta	371.9	79.4	-2.23
Postn	3,636.4	790.5	-2.20
MMP13	194.3	46.9	-2.05
Col18a1	23893.3	6450.0	-1.89
Prss34	105.6	29.6	-1.83
Fbn2	5761.4	1633.8	-1.82
Serpine1	4682.1	1457.0	-1.68
Tnc	730.5	230.3	-1.67
Col6a3	3845.8	1217.6	-1.66
Tgm2	6,632.9	2106.2	-1.65
Lama4	6488.1	2158.9	-1.59
Vwf	564.8	190.9	-1.57
MMP25	56.6	19.6	-1.53
Col11a1	11811.0	4091.6	-1.53
Spp1	4114.5	1447.0	-1.51
MMP15	13361.0	4702.4	-1.51
Col18a1	11202.6	3987.7	-1.49
Hspg2	67.3	24.4	-1.46
Hapln3	2826.7	1027.1	-1.46
Col16a1	17227.8	6288.7	-1.45
Ntn1	3002.7	1125.8	-1.42
Hapln3	2010.1	775.2	-1.37
Col4a3	47.9	18.6	-1.36
Adamts1	9047.5	3540.1	-1.35
Smoc1	6783.5	2657.7	-1.35
Bcl3	8316.9	3259.9	-1.35
Col7a1	8169.2	3347.1	-1.29
Lgals1	29926.5	12376.3	-1.27
Pdgfra	55328.5	22920.6	-1.27
Fgf1	91.6	38.5	-1.25
Gpc2	361.1	151.8	-1.25
Rgcc	55123.5	23486.4	-1.23
Fn1	63027.6	26875.3	-1.23
Hspg2	5496.3	2356.8	-1.22
Timp1	11973.6	5,185.7	-1.21
Lgals3	18282.6	8029.3	-1.19
Adamts7	202.0	90.2	-1.16
Emilin2	4333.0	1947.4	-1.15
Mfap2	7730.5	3484.5	-1.15
Adamts9	2161.7	983.7	-1.14
Fbln5	19.5	8.9	-1.13
Adamts19	45.6	21.1	-1.11
Vit	3915.2	1839.1	-1.09
Anxa2	34650.9	16410.2	-1.08
Mfap2	1209.2	578.6	-1.06
Adamts20	34.2	16.5	-1.05
Bmp7	16383.6	7938.2	-1.05
Serpine2	13500.2	6567.3	-1.04
Bmp1	3445.1	1678.4	-1.04
Sh3pxd2b	1663.0	810.2	-1.04
MMP3	396.1	198.4	-1.00

Growth factor activity

Gene	WT	GD3S-KO	Ratio
Ambn	61.1	6.2	-3.30
Tff1	67.7	17.9	-1.92
Il4	70.2	26.4	-1.41
Csf1	576.5	226.2	-1.35
Mdk	7189.2	2887.5	-1.32
Il6	180.4	74.8	-1.27
Gdnf	830.2	345.9	-1.26
Fgf1	91.6	38.5	-1.25
Fgf23	18.4	8.2	-1.16
Il4	58.2	26.6	-1.13
Wisp2	367.9	169.6	-1.12
Tgfa	802.1	378.8	-1.08
Bmp7	16383.6	7938.2	-1.05
Cxcl1	278.1	135.1	-1.04
Bmp1	3445.1	1678.4	-1.04
Inhbc	11.9	5.8	-1.03
Wisp3	88.9	43.6	-1.03
Vegfa	13195.9	6588.7	-1.00

MAPK activity

Gene	WT	GD3S-KO	Ratio
Trib1	75.0	14.5	-2.37
Nox4	640.4	184.2	-1.80
Trib3	3143.5	1135.3	-1.47
Mapk12	2,842.7	1072.1	-1.41
Nox4	344.1	131.6	-1.39
Ezh2	5874.6	2407.4	-1.29
Htr2b	115.3	54.6	-1.08
Spry4	1158.4	549.5	-1.08
Bmp7	16383.6	7938.2	-1.05

Protein tyrosine kinase activity

Gene	WT	GD3S-KO	Ratio
Flt4	35.2	12.0	-1.56
Ttk	393.4	136.7	-1.53
Melk	3574.9	1280.0	-1.48
Pdgfra	55328.5	22920.6	-1.27
Tnk1	91.3	39.0	-1.23
Styk1	25.4	10.8	-1.23
Peak1	62.6	27.1	-1.21
Erbb3	90.2	43.9	-1.04
Ripk2	64.1	31.3	-1.03
Afap1l2	7332.7	3626.9	-1.02

Ratio (Log2)

-1.0 -1.5 -2.0 -3.0

Higher expression in wild type

FIGURE 3 Lack of GD3 synthase (GD3S) resulted in altered ratios of gene expression levels in gliomas. Total RNA samples from gliomas generated in GD3S-KO or WT mice at 2 wk after injection of PDGFB-T2A-GFP-expressing cells by replication-competent avian leukemia virus splice acceptor were analyzed by DNA microarray. Lists of genes, showing ratios in gene expression intensities categorized into cell cycle, MAPK activity, growth factor activity, ECM, or protein tyrosine kinase activity. A larger ratio with minus value indicates stronger expression in control mice than in GD3S-KO mice. Glioma samples from GD3S-KO and control mice (n = 5 each) were pooled and analyzed

3.3 | Lack of GD3S resulted in alteration of gene expression profiles in gliomas

To characterize gliomas generated in GD3S-KO mice in details, we compared gene expression patterns between gliomas generated in GD3S-KO mice and those in control mice by DNA microarray. Pooled RNAs from each genetic background mouse group were used. Gene Ontology annotations for the cell cycle (GO:0007049), MAPK activity (GO:0000187), growth factor activity (GO:0008083), ECM (GO:0031012), and protein tyrosine kinase activity (GO:0004713)

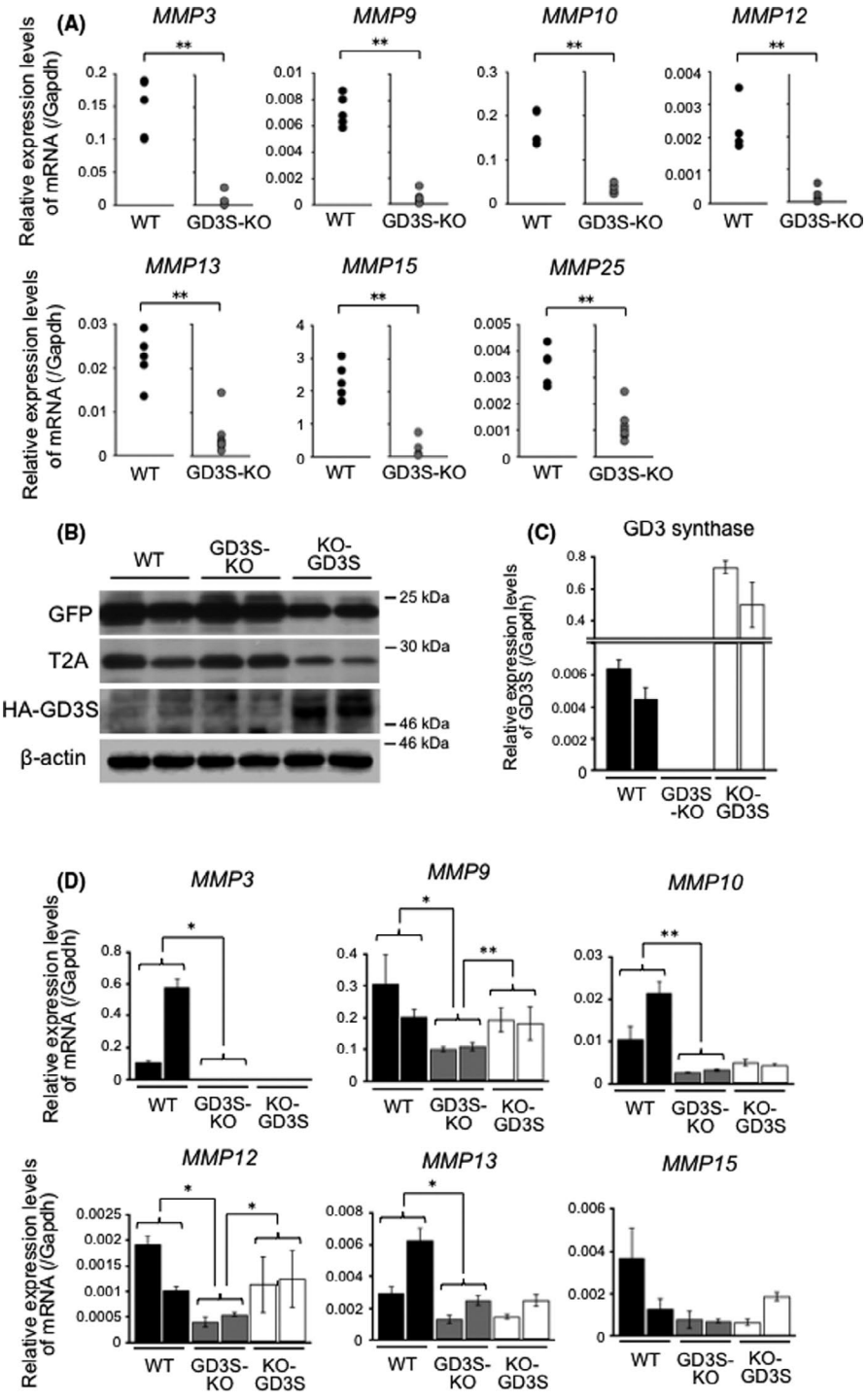

FIGURE 4 Lack of GD3 synthase (GD3S) resulted in downregulation of MMP family genes, and reexpression of GD3S resulted in restoration of MMP9/12 in glioma cells. A, Results of quantitative RT-PCR, showing relatively low mRNA levels of MMPs except MMP12 in glioma tissues generated in GD3S-KO compared with those in control mice. Samples from seven GD3S-KO and five control mice were analyzed at 2 wk after injection of PDGFB-T2A-GFP-expressing cells by replication-competent avian leukemia virus splice acceptor. Expression levels of individual genes were normalized by *Gapdh* data. $^{*}P < .05$, $^{**}P < .01$. B, Western blotting showed expression of GFP, T2A, and HA-tagged GD3S in primary-cultured glioma cells prepared from GD3S-KO and control mice. KO-GD3S indicates GD3S-KO primary-cultured glioma cells transfected with the HS-tagged *GD3S* gene. Total protein (20 μg) analyzed with Abs indicated on left side of individual images. β-Actin was used as a loading control. C, mRNA expression levels of GD3S examined by quantitative RT-PCR in primary-cultured glioma cells used in (B). Expression levels were normalized by *Gapdh* data. Error bars are SD. D, Results of quantitative RT-PCR analysis, showing relative expression levels of MMPs in primary-cultured glioma cells. Primary-cultured glioma cells prepared in (B) and (C) were analyzed. Two cell lines each were prepared from individual mice. Expression levels were normalized by *Gapdh* data. Error bars are SD. $^{*}P < .05$, $^{**}P < .01$

were carried out, and we identified a number of downregulated genes in gliomas of GD3S-KO mice compared with those of control mice by the expression levels (Figure S3) or ratios (Figure 3) between them.

Among these genes, we noted the marked downregulation of MMP family genes such as *MMP3*, *MMP9*, *MMP10*, *MMP12*, *MMP13*, *MMP15*, and *MMP25* in gliomas from GD3S-KO mice. Then we analyzed gene expression levels of MMP family members in individual glioma samples generated in GD3S-KO and control mice. As shown in Figure 4A, gliomas generated in GD3S-KO mice showed low mRNA levels of *MMP*s compared with those in control mice, corresponding with microarray data (Figure 3). Generally, high expression levels of MMP family genes are required for cancer cell invasion. Therefore, low expression levels of MMP family genes might result in weak invasion activity of glioma cells in GD3S-KO mice.

3.4 | Reintroduction of GD3S restores *MMP9* expression in glioma cells

Then, we tried to identify which *MMP*s are upregulated by GD3S by reintroducing GD3S in gliomas generated in GD3S-KO mice. We analyzed three each of primary-cultured glioma lines prepared from control mice, GD3S-KO, and GD3S-KO cells reintroduced with GD3S (Figures 4B,C and S4). Interestingly, in the expression analysis of *MMP*s using these three kinds of primary-cultured glioma cells, reintroduction of GD3S in glioma cells induced restoration of *MMP9* and *MMP12* (Figure 4D). Actually, there was no significant difference in *MMP12* expression levels between glioma tissues generated in GD3S-KO mice and control mice (Figure 4A). Consequently, only *MMP9* was identified as a consistently upregulated gene by GD3/GD2 and/or GD3S in gliomas.

3.5 | High expression of MMP9 contributes to strong invasion activity of glioma cells

To determine how MMP9 expression is associated with malignant tumor phenotypes, we undertook gelatin zymography and an invasion assay using primary-cultured glioma lines prepared from control mice and GD3S-KO mice. Interestingly, primary-cultured glioma cells prepared from control mice showed stronger gelatinase activity and invasion activity than those from GD3S-KO mice (Figure 5A). Additionally, the strong invasion activity of primary-cultured glioma cells prepared from control mice was attenuated by MMP9 inhibition (Figure 5B). Inhibition of MMP9 also changed the shape of invaded cells from amoeboid-like to round, which could be involved in the attenuation of invasion activity (Figure 5C). These data suggest that strong MMP9 expression induced by GD3/GD2 and/or GD3S contributes to the malignant phenotypes of glioma cells, such as marked invasiveness.

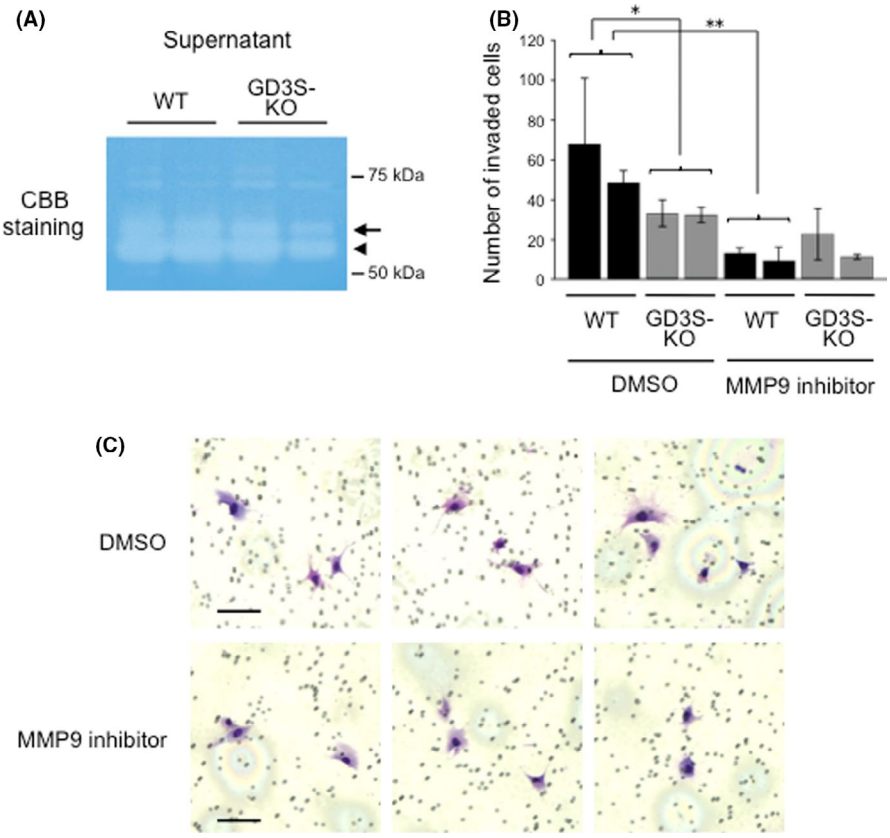

FIGURE 5 Lack of GD3 synthase (GD3S) attenuated invasiveness of glioma cells. A, Gelatin zymography shows stronger MMP9/MMP2 activity (gelatinase activity) in primary-cultured glioma cells prepared from control mice (WT) compared to GD3S-KO mice. The supernatant including 5 μg total protein was analyzed. Gelatinase activity of the C-terminal truncated MMP9 (65 kDa, arrow) and MMP2 (60 kDa, arrowhead) were observed. B, Invasion activity of primary-cultured glioma cells prepared from control mice (WT) and GD3S-KO mice in the presence or absence of MMP9 inhibitor I (20 μmol/L). Invaded cells were counted after incubation for 24 h. Two cell lines each prepared from individual mice were analyzed. Error bars are SD. $^{*}P < .05$, $^{**}P < .01$. C, Three representative images each of invaded cells prepared from control mice (WT) under presence or absence of MMP9 inhibitor I (20 μmol/L). Bars, 100 μm

3.6 | Transcription factor Ap2α upregulates *MMP9* in astrocytes

To clarify mechanisms for the upregulation of *MMP9* in GD3S-expressing gliomas, we focused on transcription factors that have been reported as candidate regulators of *MMP9* expression, such as Ap2α[15] Sp1,[16] Ap1 (c-Fos, c-Jun),[17] and Nfkb (p65, Nfkb2).[18] Among them, Ap2α, Sp1, and p65 showed significantly higher levels in GD3$^+$ astrocytes (Figure 6A). In particular, Ap2α showed markedly higher levels in GD3$^+$ cells than in GD3$^-$ cells. When expression levels of Ap2α were compared in glioma and nonglioma tissues from GD3S-KO and control mice, Ap2α was also expressed more strongly in gliomas in control mice than in GD3S-KO mice (Figure 6B). Ap1 (c-Fos, c-Jun) and Nfkb2 were highly expressed in gliomas in control mice compared with GD3S-KO mice. However, their expression patterns were not parallel with GD3 expression in astrocytes, as shown in Figure 6A. For this reason, we identified Ap2α as a candidate regulator of *MMP9* expression under GD3 expression. We also detected higher expression levels of *MMP3*, *MMP9*, and *MMP12* in GD3$^+$ astrocytes than in GD3$^-$ astrocytes (Figure S5).

There are two well-characterized kinds of splicing variants for murine Ap2α, tv1 (NM_011547.4) and tv3 (NM_001122948.2).[19] We overexpressed these two variants to examine which Ap2α variant drives the *MMP9* gene. As we expected, forced expression of Ap2α, especially Ap2α tv3, resulted in increased *MMP9* gene expression in three individual primary-cultured astrocytes (Figure 7A,B). The effects of these factors on the expression of other MMP family members were also analyzed, resulting in similar but less intense effects on MMP3 and MMP10 (Figure 7C).

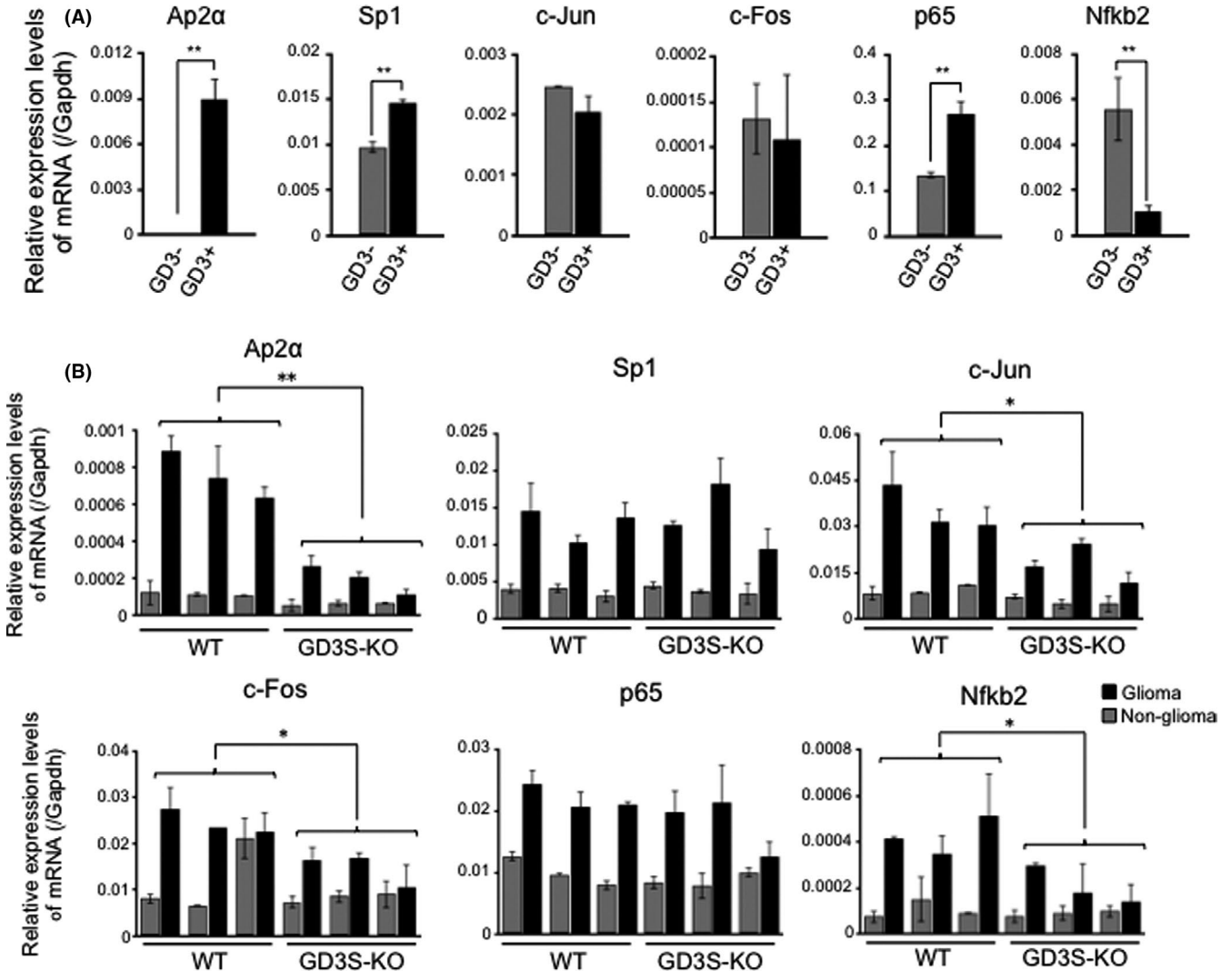

FIGURE 6 Expression of transcription factor Ap2α in astrocytes and gliomas. A, mRNA expression levels for *Ap2α*, *Sp1*, *c-Jun*, *c-Fos*, *p65*, and *Nfkb2* in GD3-expressing and GD3$^-$ astrocytes prepared from PDGFB cDNA-transfected primary-cultured astrocytes. Gene expression levels were analyzed by quantitative RT-PCR (qRT-PCR) and normalized by *Gapdh* data. *$P < .05$, **$P < .01$. B, Results of qRT-PCR to examine mRNA expression levels for *Ap2α*, *Sp1*, *c-Jun*, *c-Fos*, *p65*, and *Nfkb2* in glioma (black bars) and nonglioma tissues (gray bars) of the brain. Samples were prepared from three each of GD3S-KO and control mice at 2 wk after injection of PDGFB-T2A-GFP cDNA-expressing cells. Relative expression levels were normalized by *Gapdh* data. **$P < .01$

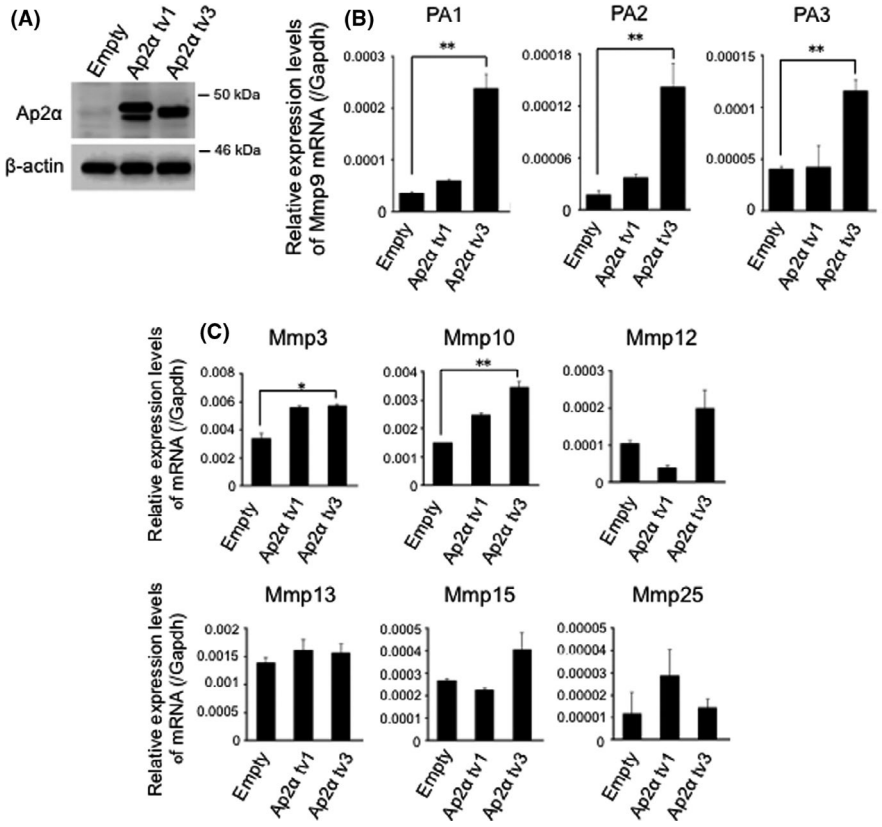

FIGURE 7 Transcription factor Ap2α tv3 upregulates *MMP9*. A, Ap2α protein expression levels in primary-cultured astrocytes. After transfection of Ap2α splicing variant 1 (tv1) and variant 3 (tv3) or PDGFB-T2A-GFP cDNA, total proteins (20 μg) were analyzed by western blotting with anti-Ap2α Ab or anti-T2A peptide Ab. β-Actin was used as a loading control. B, *MMP9* gene expression levels after transfection with Ap2α tv1, Ap2α tv3, or PDGFB-T2A-GFP cDNA of primary-cultured astrocytes. Three primary-cultured astrocytes (PA1, PA2, and PA3) from three individual control mice were examined. Expression levels of *MMP9* were normalized by *Gapdh* data. $^{**}P < .01$. Error bars are SD. C, Gene expression levels of *MMP3*, *MMP10*, *MMP12*, *MMP13*, *MMP15*, and *MMP25* in primary-cultured astrocytes after transfection with Ap2α tv1, Ap2α tv3, or PDGFB-T2A-GFP cDNA. Gene expression levels were analyzed by quantitative PCR and normalized by *Gapdh* data. $^{*}P < .05$, $^{**}P < .01$. Error bars are SD

3.7 | Transcription factor Ap2α tv3 binds and drives *MMP9* promoter in astrocytes

Furthermore, we examined whether Ap2α actually binds to the MMP9 promoter and promotes expression of the MMP9 gene by ChIP-PCR and luciferase assay, respectively. Using four primer sets designed around two Ap2α binding sequences (Figure 8A), ChIP-PCR analysis was carried out and revealed evidence of binding of the transcription factor Ap2α tv3 to regions near primer sites 3 and 4 of the *MMP9* gene promoter (Figure 8B). Ap2α tv1 also showed similar, but much weaker binding than Ap2α tv3. The luciferase reporter assay revealed that Ap2α tv3 drove transcription of *MMP9* (Figure 8C). Taken together, activation of signaling pathways and upregulation of *MMP9* induced via Ap2α based on GD3/GD2 and/or GD3S expression actually promoted the progression of gliomas.

As shown in Figure 9A, GD3S-KO mice with the introduction of GD3S cDNA together with the PDGFB expression vector tended to show a shorter survival than GD3S KO mice. In Figure 9B, the conclusion of this study is summarized. Activation of Akt, SFKs, and Erks and upregulation of MMP9 by Ap2α lead to emergence of malignant phenotypes in gliomas under the expression of GD3/GD2 and/or GD3S.

4 | DISCUSSION

Gangliosides are localized in lipid rafts of the cell membrane and function as a fine tuner of cell signals by modulating properties of lipid rafts.[20] Gangliosides including GD3 and GD2 are required for neurogenesis,[21] and play a protective role in neuroinflammation.[22] In cancer cells, high and specific expression of ganglioside GD3 and/or GD2 enhances cell signals, resulting in malignant phenotypes such as rapid cell growth and increased invasiveness, as shown in small-cell lung cancer cells.[23] GD3 also enhances adhesion signals and phosphorylation levels of adaptor molecules such as p130Cas and paxillin in melanomas.[24,25] Although expression of GD3 and/or GD2 enhanced malignant properties in tumors, as reported,[26] there are few reports describing how GD3 and GD2 play roles in tumorigenesis and tumor progression in vivo. In this study, we found that loss of GD3S resulted in the reduction of phosphorylation levels of Akt,

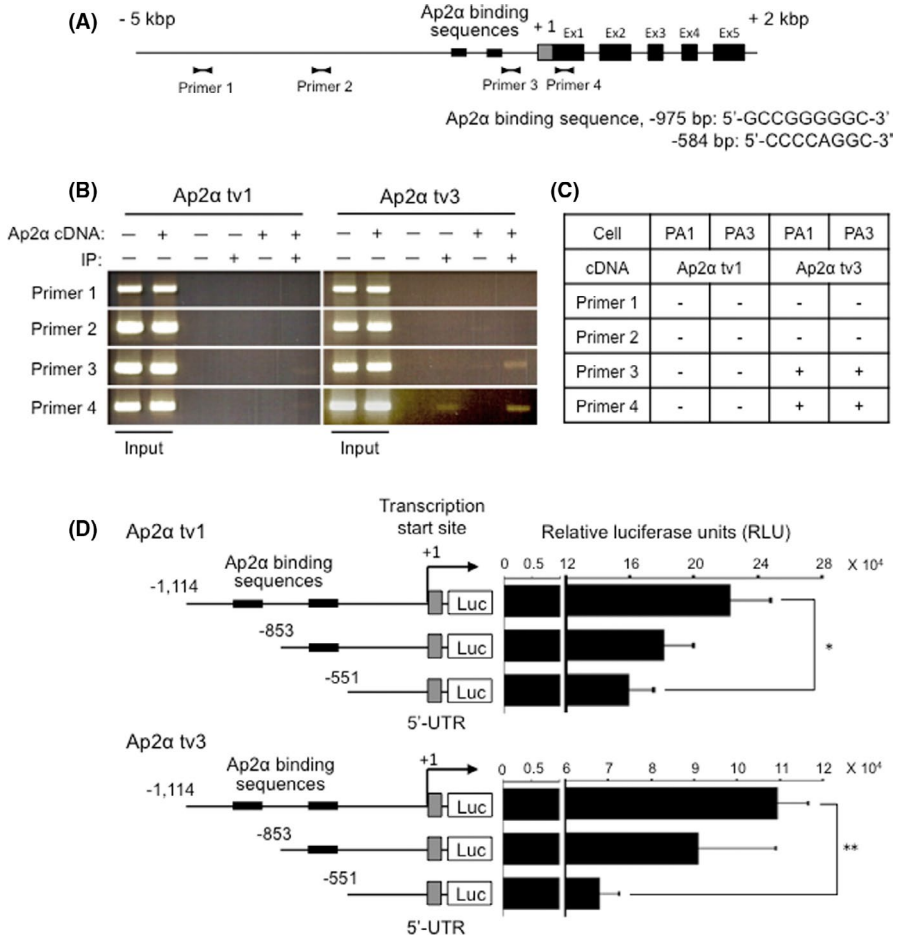

FIGURE 8 Ap2α binds *MMP9* promoter and functions in astrocytes. A, Genomic structure of the murine MMP9 promoter region. Putative transcription start site is shown as +1. The genomic region indicated by a gray box is the 5′-UTR and thick boxes indicate exons. Two Ap2α binding sequences are located at −584 and −975, and four sets of PCR primers were prepared in the upstream region and exon 1 of the *MMP9* gene, as shown in the figure. B, Results of PCR using ChIP samples. After transfection with Ap2α tv1 or Ap2α tv3 cDNA of primary-cultured astrocytes (PA3), ChIP was undertaken with an anti-Ap2α Ab. DNAs in immunoprecipitates were purified and PCR was subsequently carried out with primers described in (A). An empty vector was used for transfection as a control, and nonrelevant IgG was used as a control for immunoprecipitation. C, Summary of band intensities for ChIP-PCR in primary-cultured astrocyte PA1 and PA3. Cells were transfected with Ap2α tv1 or Ap2α tv3 cDNA, then ChIP-PCR was carried out with an anti-Ap2α Ab and primers described in (A). +, strong; −, no band. D, Dual luciferase assay (*Photinus pyralis* luciferase and *Renilla reniformis* luciferase) was carried out, and the results are shown as promoter activity of MMP9 promoter after cotransfection with Ap2α tv1 or Ap2α tv3 with pGL3/MMP9 promoter vectors in primary-cultured astrocytes (PA3). Three kinds of vectors containing two, one, or no Ap2α-binding sequences were used. Thick lines, Ap2α binding sequences; Luc, luciferase gene. $^{*}P < .05$, $^{**}P < .01$. Error bars are SD

SFKs, and Erks in gliomas, indicating that oncogenic cell signals were attenuated due to lack of expression of GD3 and/or GD2 in gliomas (Figures 1 and 2). Interestingly, lack of GD3S dynamically altered expression profiles of a wide variety of genes in gliomas, as presented in Figure 3. Among them, we identified several *MMP* family genes as markedly downregulated in gliomas lacking GD3S.

There are 25 known MMPs in mammals. They are proteases targeting several kinds of proteins included in the ECM such as collagens, elastin, and gelatin. Among MMPs, MMP9 is frequently overexpressed in cancers and required for invasion of cancer cells.[27] Importantly, other groups reported that PI3K/AKT and MAPK pathways were essential for MMP activity as well as invasiveness in glioma cells. The association between an increased PI3K/AKT pathway and increased MMP9 activity and invasiveness was described.[28] Furthermore, it was also reported that activation of the Raf1-MEK-ERK pathway induces MMP9 activity and enhances invasion activity.[29] These studies strongly suggest that PI3K/AKT and MAPK pathways should be targeted to suppress the growth and invasiveness of glioma cells. Based on our findings, MMP9 expression levels were restored by re-expression of GD3S in GD3^{-} cells (Figure 4D), indicating that GD3/GD2-expressing gliomas have high potential for invasiveness through MMP9. Moreover, we identified the transcription factor Ap2α as a key regulator for upregulation of *MMP9* (Figures 6-8). Although the expression and function of Ap2α in gliomas and other tumors have been reported, it is controversial whether Ap2α positively modulates the malignant properties of

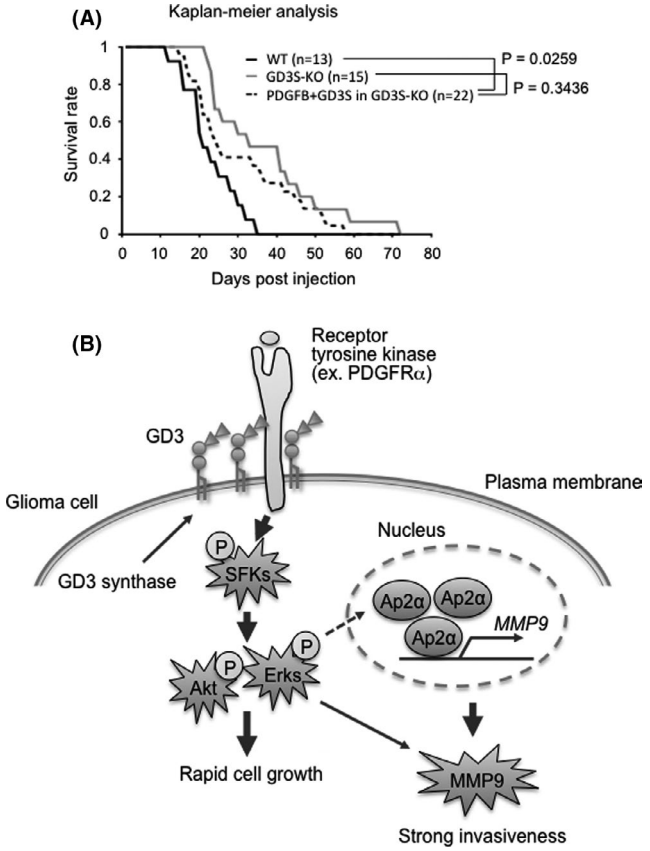

FIGURE 9 Survival curves of GD3 synthase (GD3S)-KO injected with GD3S expression vectors. A, Kaplan-Meier analysis showing that GD3S-KO mice injected with GD3S together with platelet-derived growth factor B (PDGFB) expression vector (22 mice) tended to show a shorter survival time than GD3S-KO mice ($P = .3436$, log-rank test). Other data such as simple transfection with PDGFB cDNA in GD3S-KO and control mice were the same as those presented in Figure 1B, showing longer survival of GD3S-KO mice than WT mice. B, Summary of the conclusion of this study. Activation of Akt, Src family kinase (SFKs), and Erks and upregulation of MMP9 by Ap2α lead to malignant phenotypes of gliomas under expression of GD3/GD2 and/or GD3S. The mechanism of how GD3S induces strong expression of Ap2α remains to be investigated. PDGFRα, platelet-derived growth factor receptor α

tumors.[30-32] Differential functions for each variant of Ap2α have not been well-clarified, whereas sumoylation, which occurs only in Ap2α tv1, might be involved in the regulation of Ap2α tv3 and *MMP9* gene expression in gliomas.[33] Our results showing that Ap2α tv3 bound and drove the *MMP9* promoter could be novel and meaningful when considering precise Ap2α functions in gliomas. However, it remains to be clarified how GD3/GD2 and/or GD3S regulate transcriptional activity of Ap2α in gliomas.

Ganglioside GD3 has been considered to be a marker of neuroprogenitor cells[34] due to its dominant expression in neuronal cells at E12-14 days in mice.[35] However, GD3S-deficient mice show almost normal development of nervous tissues,[11] suggesting that b-series gangliosides are not indispensable for neurogenesis. In turn, GD3 and/or GD2 have been analyzed regarding roles in various cancers, and a number of studies have reported their enhancing effects on many signaling molecules associated with cell growth, migration, invasion, and metastasis. However, many of them have been analyzed using cultured cells.[26] Although GD3/GD3 synthase was reported as a key molecule to maintain glioma stem cells,[36] the evidence was based on experiments in vitro. Therefore, the results reported here show the novel impact on the essential roles of GD3/GD2 in gliomagenesis and progression in vivo. Although major signaling pathways promoting malignant properties, such as increased cell growth and invasiveness, in glioma tissues under GD3 expression were described here and in previous reports,[8] cross-talk between the PDGFR2α-Yes-paxillin pathway and the Ap22α-MMP9 axis remains to be clarified. AS GD3- and/or GD2-targeted therapies for neural crest-derived tumors have been long attempted and are now under development,[7] our results could suggest novel targets for cancer therapeutics of signaling pathways activated by cancer-associated gangliosides, as we reported recently.[37,38]

ACKNOWLEDGMENTS

We thank S. Yamamoto and Y. Nakayasu for technical assistance. This study was supported by Grants-in-Aids of the Ministry of Education, Culture, Sports and Technology of Japan (MEXT) (15H04696, 25670141, 24390078, 23110008, and 20K07629), and by JST-CREST (Grant Number: JPMJCR17H2).

DISCLOSURE

The authors declare no conflict of interest.

ORCID

Atsushi Natsume https://orcid.org/0000-0002-9113-0470
Koichi Furukawa https://orcid.org/0000-0002-3321-9784

REFERENCES

1. Huse JT, Holland EC. Targeting brain cancer: advances in the molecular pathology of malignant glioma and medulloblastoma. *Nat Rev Cancer*. 2010;10:319-331.
2. Wen PY, Kesari S. Malignant gliomas in adults. *N Engl J Med*. 2008;359:492-507.
3. Wang Q, Hu B, Hu X, et al. Tumor evolution of glioma-intrinsic gene expression subtypes associates with immunological changes in the microenvironment. *Cancer Cell*. 2017;32:42-56.e6.
4. Lloyd KO, Gordon CM, Thampoe IJ, DiBenedetto C. Cell surface accessibility of individual gangliosides in malignant melanoma cells to antibodies is influenced by the total ganglioside composition of the cells. *Cancer Res*. 1992;52:4948-4953.
5. Wagener R, Röhn G, Schillinger G, Schröder R, Kobbe B, Ernestus RI. Ganglioside profiles in human gliomas: quantification by microbore high performance liquid chromatography and correlation to histomorphology and grading. *Acta Neurochir (Wien)*. 1999;141:1339-1345.
6. Cheresh DA, Rosenberg J, Mujoo K, Hirschowitz L, Reisfeld RA. Biosynthesis and expression of the disialoganglioside GD2, a relevant target antigen on small cell lung carcinoma for monoclonal antibody-mediated cytolysis. *Cancer Res*. 1986;46:5112-5118.
7. Heimburg-Molinaro J, Lum M, Vijay G, Jain M, Almogren A, Rittenhouse-Olson K. Cancer vaccines and carbohydrate epitopes. *Vaccine*. 2011;29:8802-8826.

8. Ohkawa Y, Momota H, Kato A, et al. Ganglioside GD3 enhances invasiveness of gliomas by forming a complex with platelet-derived growth factor receptor α and yes kinase. *J Biol Chem*. 2015;290:16043-16058.
9. Hambardzumyan D, Amankulor NM, Helmy KY, Becher OJ, Holland EC. Modeling adult gliomas using RCAS/t-va technology. *Transl Oncol*. 2009;2:89-95.
10. Huse JT, Holland EC. Genetically engineered mouse models of brain cancer and the promise of preclinical testing. *Brain Pathol*. 2009;19:132-143.
11. Okada M, Itoh Mi M, Haraguchi M, et al. b-series Ganglioside deficiency exhibits no definite changes in the neurogenesis and the sensitivity to Fas-mediated apoptosis but impairs regeneration of the lesioned hypoglossal nerve. *J Biol Chem*. 2002;277:1633-1636.
12. Zhao J, Furukawa K, Fukumoto S, et al. Attenuation of interleukin 2 signal in the spleen cells of complex ganglioside-lacking mice. *J Biol Chem*. 1999;274:13744-13747.
13. Kim JH, Lee S-R, Li L-H, et al. High cleavage efficiency of a 2A peptide derived from porcine teschovirus-1 in human cell lines, zebrafish and mice. *PLoS One*. 2011;6:e18556. https://doi.org/10.1371/journal.pone.0018556
14. Grzmil M, Hemmings BA. Deregulated signalling networks in human brain tumours. *Biochim Biophys Acta*. 2010;1804:476-483.
15. Schwartz B, Melnikova VO, Tellez C, et al. Loss of AP-2alpha results in deregulation of E-cadherin and MMP-9 and an increase in tumorigenicity of colon cancer cells in vivo. *Oncogene*. 2007;26:4049-4058.
16. Murthy S, Ryan AJ, Carter AB. SP-1 regulation of MMP-9 expression requires Ser586 in the PEST domain. *Biochem J*. 2012;445:229-236.
17. Ray A, Bal BS, Ray BK. Transcriptional induction of matrix metalloproteinase-9 in the chondrocyte and synoviocyte cells is regulated via a novel mechanism: evidence for functional cooperation between serum amyloid A-activating factor-1 and AP-1. *J Immunol*. 2005;175:4039-4048.
18. Rhee JW, Lee K-W, Sohn W-J, et al. Regulation of matrix metalloproteinase-9 gene expression and cell migration by NF-kappa B in response to CpG-oligodeoxynucleotides in RAW 264.7 cells. *Mol Immunol*. 2007;44:1393-1400.
19. Meier P, Koedood M, Philipp J, Fontana A, Mitchell PJ. Alternative mRNAs encode multiple isoforms of transcription factor AP-2 during murine embryogenesis. *Dev Biol*. 1995;169:1-14.
20. Hakomori S, Yamamura S, Handa AK. Signal transduction through glyco(sphingo)lipids. Introduction and recent studies on glyco(sphingo)lipid-enriched microdomains. *Ann N Y Acad Sci*. 1998;845:1-10.
21. Wang J, Cheng A, Wakade C, Yu RK. Ganglioside GD3 is required for neurogenesis and long-term maintenance of neural stem cells in the postnatal mouse brain. *J Neurosci*. 2014;34:13790-13800.
22. Ohmi Y, Tajima O, Ohkawa Y, et al. Gangliosides are essential in the protection of inflammation and neurodegeneration via maintenance of lipid rafts: elucidation by a series of ganglioside-deficient mutant mice. *J Neurochem*. 2011;116:926-935.
23. Yoshida S, Fukumoto S, Kawaguchi H, Sato S, Ueda R, Furukawa K. Ganglioside G(D2) in small cell lung cancer cell lines: enhancement of cell proliferation and mediation of apoptosis. *Cancer Res*. 2001;61:4244-4252.
24. Ohkawa Y, Miyazaki S, Hamamura K, et al. Ganglioside GD3 enhances adhesion signals and augments malignant properties of melanoma cells by recruiting integrins to glycolipid-enriched microdomains *. *J Biol Chem*. 2010;285:27213-27223.
25. Hamamura K, Furukawa K, Hayashi T, et al. Ganglioside GD3 promotes cell growth and invasion through p130Cas and paxillin in malignant melanoma cells. *Proc Natl Acad Sci U S A*. 2005;102:11041-11046.
26. Furukawa K, Ohkawa Y, Matsumoto Y, Ohmi Y, Hashimoto N, Furukawa K. Regulatory Mechanisms for Malignant Properties of Cancer Cells with Disialyl and Monosialyl Gangliosides. In: Furukawa K, Fukuda M, eds. *Glycosignals in Cancer: Mechanisms of Malignant Phenotypes*. Tokyo, Japan: Springer; 2016:57-76.
27. Farina AR, Mackay AR. Gelatinase B/MMP-9 in tumour pathogenesis and progression. *Cancers (Basel)*. 2014;6:240-296.
28. Kubiatowski T, Jang T, Lachyankar MB, et al. Association of increased phosphatidylinositol 3-kinase signaling with increased invasiveness and gelatinase activity in malignant gliomas. *J Neurosurg*. 2001;95:480-488.
29. Das G, Shiras A, Shanmuganandam K, Shastry P. Rictor regulates MMP-9 activity and invasion through Raf-1-MEK-ERK signaling pathway in glioma cells. *Mol Carcinog*. 2011;50:412-423.
30. Schulte JH, Kirfel J, Lim S, et al. Transcription factor AP2alpha (TFAP2a) regulates differentiation and proliferation of neuroblastoma cells. *Cancer Lett*. 2008;271:56-63.
31. Orso F, Penna E, Cimino D, et al. AP-2alpha and AP-2gamma regulate tumor progression via specific genetic programs. *FASEB J*. 2008;22:2702-2714.
32. Huang W, Chen C, Liang Z, et al. AP-2α inhibits hepatocellular carcinoma cell growth and migration. *Int J Oncol*. 2016;48:1125-1134.
33. Bogachek MV, Chen Y, Kulak MV, et al. Sumoylation pathway is required to maintain the basal breast cancer subtype. *Cancer Cell*. 2014;25:748-761.
34. Wang J, Yu RK. Interaction of ganglioside GD3 with an EGF receptor sustains the self-renewal ability of mouse neural stem cells in vitro. *Proc Natl Acad Sci USA*. 2013;110:19137-19142.
35. Ngamukote S, Yanagisawa M, Ariga T, Ando S, Yu RK. Developmental changes of glycosphingolipids and expression of glycogenes in mouse brains. *J Neurochem*. 2007;103:2327-2341.
36. Yeh S-C, Wang P-Y, Lou Y-W, et al. Glycolipid GD3 and GD3 synthase are key drivers for glioblastoma stem cells and tumorigenicity. *Proc Natl Acad Sci USA*. 2016;113:5592-5597.
37. Furukawa K, Hamamura K, Aixinjueluo W, Furukawa K. Biosignals modulated by tumor-associated carbohydrate antigens: novel targets for cancer therapy. *Ann N Y Acad Sci*. 2006;1086:185-198.
38. Makino Y, Hamamura K, Takei Y, et al. A therapeutic trial of human melanomas with combined small interfering RNAs targeting adaptor molecules p130Cas and paxillin activated under expression of ganglioside GD3. *Biochim Biophys Acta*. 2016;1860:1753-1763.

SUPPORTING INFORMATION

Additional supporting information may be found online in the Supporting Information section.

How to cite this article: Ohkawa Y, Zhang P, Momota H, et al. Lack of GD3 synthase (St8sia1) attenuates malignant properties of gliomas in genetically engineered mouse model. *Cancer Sci*. 2021;112:3756–3768. https://doi.org/10.1111/cas.15032